

Localized breathing solutions for Bose-Einstein condensates in periodic traps.

R. Carretero-González* and K. Promislow

Department of Mathematics & Statistics, Simon Fraser University, Burnaby, BC, V5A 1S6, Canada

(Submitted to *Phys. Rev. Lett.*, May 30, 2001. For related works visit <http://www.math.sfu.ca/~rcarretero/abstracts.html>)

We demonstrate the existence of localized oscillatory breathers for quasi-1D Bose-Einstein condensates confined in periodic potentials. Localized oscillations are identified with a homoclinic tangle of a 2D map on the oscillation amplitudes. This construction implies structural stability of the localized breathers to parameter tuning and external noise. We also predict the existence of periodic and chaotic extended oscillations of the condensates. The regimes we consider are compatible with current physical parameter values, opening the possibility for experimental corroboration.

PACS numbers: 5.45.-a, 03.75.Fi, 52.35.Mw, 63.20.Pw

New techniques for generating Bose-Einstein condensates (BECs) have opened the door to the investigation of a wide range of phenomena and development of concrete applications such as atomic interferometers and atom lasers. Recent focus has been on BECs trapped in periodic magnetic/optical traps [1], the so-called optical lattice [2]. The addition of a periodic potential to the dynamics of the BEC opens the possibility to exciting phenomena such as Bloch oscillations and the Josephson effect [1]. In this letter we report novel solutions for the dynamics of interacting condensates in a periodic trap with widely spaced wells. For experimentally realizable regimes we reduce the BEC dynamics to a lattice differential equation and establish the existence of global and localized oscillations of the coupled condensates. The existence of localized breathers demonstrates the ability of condensates to store macroscopic information in particular regions of the periodic trap.

The macroscopic mean field of dilute BECs is governed by the Gross-Pitaevskii equation (GPE) [3]. In three space dimensions, the GPE takes the form of a cubic, time dependent, nonlinear Schrödinger equation (NLSE) with an external potential due to the trap. When the longitudinal direction is much larger than the transverse dimension (of the order of the healing length) the GPE reduces to the 1D NLSE in the quasi-1D regime [4]. We limit our study to these one-dimensional models of BECs.

In the quasi-1D regime, the BEC trapped inside a periodic potential V is governed by the NLSE, which in dimensionless units takes the form

$$iu_t + \frac{1}{2}u_{xx} \pm |u|^2u = V(x)u. \quad (1)$$

Here $u(x, t)$ is the mean field density of the condensate and the \pm sign corresponds to attractive (+) and repulsive (−) atoms. The nondimensionalization is obtained by scaling $t \rightarrow \Omega t$, $x \rightarrow (\hbar/2\Omega)^{-1/2}x$ and $|u|^2 \rightarrow (4\pi\hbar\mathcal{N}|a|/M\Omega)|u|^2$ where \mathcal{N} is the number of condensed atoms, M is the atomic mass, Ω is the frequency of the periodic trap and a is the s -wave scattering length [5]. We consider a periodic potential $V(x)$, with well spaced troughs, constructed by ‘concatenating’

single well potentials $V_j(x) = V_0 \tanh^2(x - \xi_{0;j})$:

$$V(x) = \sum_{j=-N}^N V_j(x) - 2N V_0.$$

The potentials are located at $\xi_{0;j} = jR$ where R is the potential well spacing. The specific shape of the potentials V_j is not central to the construction. However, our approximations require that neighboring condensates, grown in adjacent wells, have small overlap. This regime corresponds to large R or to a small number of atoms per potential well. The large R limit can be achieved using an optical trap with large wavenumber. Alternatively, new advances in the manipulation of condensates permit the construction of traps with arbitrary spatial patterns by imprinting the pattern in a crystal by a grating method or by lithography [6].

The present letter addresses the dynamics of a chain of coupled attractive condensates, ie. *bright* solitons. For repulsive atoms —*dark* solitons [7]— a similar approach is possible and the detailed analysis will be carried elsewhere. Current typical lifetimes for attractive condensates range from hundreds to tenths of a second before collapse. These lifetimes correspond, for typical experimental parameters in ^{85}Rb [8], to 10^3 rescaled times units which is long enough to observe localized oscillations over 10–20 oscillation periods. Moreover, new microtrap techniques [6] and hollow lasers traps [9] hold out the possibility to increase considerably the lifetime of attractive condensates [10], permitting time to prepare the train of condensates with the desired phase configuration. It is also important to note that collapse for attractive condensates can be arrested by controlling the number of atoms. Indeed, if the number of atoms is smaller than N_{cr} collapse is avoided (N_{cr} is of the order of 1000 for ^7Li) [11]. In our model it suffices that the number of atoms in *each* potential trough is smaller than N_{cr} .

The steady state for a single condensate inside a single well potential V_j is a NLSE soliton solution of the form $u_{0;j}(x, t) = \sqrt{1 - V_0} \text{sech}(x - \xi_{0;j}) e^{i(1/2 - V_0)t}$ [12]. We consider the dynamics of a train of condensates $u(x, t) = \sum u_{0;j}(x, t)$ centered at the potential troughs

$\xi_{0;j}$. For simplicity of presentation, we approximate the overall dynamics, focusing on two major contributions: a) internal dynamics due to interactions between $u_{0;j}$ and V_j and b) tail-tail interactions between consecutive solitons. We address each of these terms individually and use the linear superposition afforded by soliton perturbation theory [13]. Within our approximations (small tail-tail overlap) it is sensible to discard interactions between $u_{0;j}$ and V_k for $j \neq k$ and interactions between non-nearest neighbor condensates [13].

The evolution, for small perturbations, of the steady state soliton $u_{0;j}$ inside its on-site potential V_j can be approximated by an oscillating soliton ansatz with constant height and width [14]. The position $\xi_j(t)$ for each condensate is then described by a particle inside an effective potential:

$$\ddot{\xi}_j = -V'_{\text{eff}}(\xi - \xi_{0;j}). \quad (2)$$

The exact form of V_{eff} depends on the on-site potential V_j . For $V_j(x) = V_0 \tanh^2(x - \xi_{0;j})$ the effective potential admits the expansion $V_{\text{eff}}(x)/V_0 = \frac{4}{15}x^2 - \frac{4}{63}x^4 + o(x^6)$. For more general on-site potentials, the effective potential can be approximated (for small oscillations) by

$$V'_{\text{eff}}(x) = \alpha x + \beta x^3 + o(x^5).$$

Tail-tail interactions for neighboring condensates result in a complex version of the Toda lattice involving position and phases [15]. It is possible to further reduce the dynamics under the assumption that relative phases for consecutive condensates are constant. This is a reasonable approximation in our regime where the solitons are kept well apart at an almost constant spacing R [16]. With a relative phase of π —chosen for stability considerations [12]—the tail-tail interactions reduce to a *real* Toda lattice (TL) [17] on the positions: $\ddot{\xi}_j = 4(e^{-(\xi_j - \xi_{j-1})} - e^{-(\xi_{j+1} - \xi_j)})$. In practice, the π phase shift can be implemented by phase design on the initial configuration of the condensates [18].

Exploiting the linearity of soliton perturbation theory we combine the on-site potential (2) with the tail-tail interactions to find a lattice differential equation (LDE) on the condensate positions

$$\ddot{\xi}_j = 4 \left(e^{-(\xi_j - \xi_{j-1})} - e^{-(\xi_{j+1} - \xi_j)} \right) - V'_{\text{eff}}(\xi_j - \xi_{0;j}). \quad (3)$$

To find oscillatory solutions to (3) we use an oscillating ansatz [19], writing the position of the j th condensate as a combination of oscillatory modes $\xi_j(t) = \sum_k A_j(k) \cos(k\omega t)$ centered at $A_j(0) = \xi_{0;j}$. For small oscillations a *one-mode* ansatz

$$\xi_j(t) = \xi_{0;j} + A_j \cos(\omega t) \quad (4)$$

is sufficient to capture the essential dynamics. We substitute (4) into (3), expand and match terms to find a recurrence relation between the oscillation amplitudes A_j :

$$A_{j+1} = (a + b A_j^2) A_j - A_{j-1}, \quad (5)$$

with $a = 2 - \omega^2 + \alpha e^R/4$ and $b = 3\beta e^R/16$. We introduce $y_n = A_n$ and $x_n = A_{n-1}$ and recast the second order recurrence relation (5) as the 2D map M :

$$M : (x_{n+1}, y_{n+1}) = (y_n, (a + b y_n^2) y_n - x_n). \quad (6)$$

Up to the approximations made to obtain equation (5), solutions of (6) prescribe the amplitudes representing oscillatory solutions for the condensates. We remark that the oscillation frequency ω and the form of the on-site potential are incorporated through the parameters a and b of (5). In particular, one expects families of oscillatory solutions parameterized by their frequency ω . It is worth mentioning that the iteration index n in (6) corresponds to the site index j for the amplitude of the oscillation (4).

We are interested in constructing *localized breathers* (localized oscillations) for the condensate dynamics. These solutions correspond to orbits homoclinic to the origin for the recurrence map (6). These orbits satisfy $A_0 \neq 0$ and $\lim_{n \rightarrow \pm\infty} A_n = 0$ with an exponential decay rate. A necessary condition for the existence of a homoclinic orbit is hyperbolicity of the origin. This is satisfied for all $|a| > 2$ or equivalently $|2 - \omega^2 + \alpha e^R/4| > 2$, which provides constraints on the inter-site spacing R and breather frequency ω for a given on-site trap V_j . We find numerically, for reasonable values of R ($R \approx$ a few condensate widths), that the stable and unstable manifolds of the origin intersect in a homoclinic tangle (see left panel in Fig. 1). The amplitudes for the localized oscillations are then given by the ordinates of the homoclinic orbit (see right panel in Fig. 1).

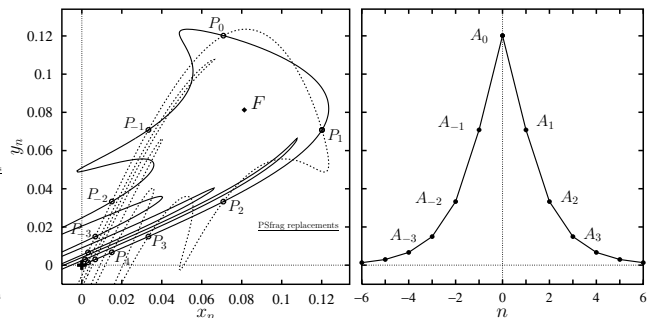


FIG. 1. Left: Homoclinic tangle for the two-dimensional map (6). The homoclinic orbit $\{\dots, P_{-1}, P_0, P_1, \dots\}$ belongs to the stable (solid line) and unstable (dash line) manifolds. Right: The corresponding configuration for the oscillation amplitudes. ($R = 10$, $\omega = 17.671$ and $V_0 = 0.1$.)

The homoclinic orbit of the 2D map induces a breather on the condensate positions through the ansatz (4). An example of such localized oscillations for the condensates is depicted in Fig. 2, in which a central condensate oscillates with a maximal amplitude A_0 and the condensates on either side oscillate with amplitudes $A_{\pm n}$ which decrease exponentially in increasing n (see right panel in Fig. 1). The asymptotic decay rate for the oscillations

($\lambda_-^{|n|} = \lambda_+^{-|n|}$) is prescribed by the eigenvalues at the origin $\lambda_{\pm} = (a \pm \sqrt{a^2 - 4})/2$. Note that, because (6) has $x \leftrightarrow y$ symmetry, the breather is symmetric with respect to the central condensate ($\lambda_- = \lambda_+^{-1}$).

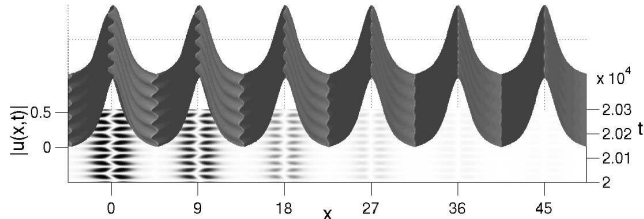


FIG. 2. Localized breathing oscillation of (1) showing the dynamics of coupled BECs in a periodic potential. Only condensates with index 0 through 5 are shown (the oscillations are symmetric with respect to the origin). The bottom plane depicts u_t — darker areas corresponds to regions where $u(x, t)$ undergoes greater temporal variation. ($R = 9$, $\omega \approx 0.11388$ and $V_0 = 0.025$.)

Localized breathers represent an important structure in the dynamics of the GPE equation describing a mechanism whereby energy and information can be pinned down on the periodic potential lattice. The occurrence of localized breathers in weakly coupled oscillatory units is a common phenomenon. Indeed, the existence of localized breathers has been formally established in general nonlinear Hamiltonian lattices of weakly interacting oscillators by continuation from the so called anticontinuum limit corresponding to the uncoupled case ($R = +\infty$) [20]. A crucial item that deserves elaborating at this point is the structural stability of the homoclinic tangle with respect to parameter changes and external perturbations. Despite the various approximations used in the reduction of the NLSE to the 2D map (6), we observe localized breather oscillations in the original NLSE dynamics (Fig. 2) for the predicted parameter values.

To stress the robustness of our construction we follow the evolution of a perturbed breather for the NLSE (Fig. 3). We construct the initial configuration (IC) as a concatenation of solitons with velocities, heights, widths and positions predicted by our analysis, and with a π phase shift between consecutive solitons (as in Fig. 2). We then introduce a perturbation to each soliton in the chain by adding a random value to each of the initial velocities, heights, widths, positions and phases. The bounds for the perturbations correspond to a) 15% of the *maximal* velocity on velocities, b) 10% on heights, c) 10% on widths, d) 15% of the *maximal* amplitude ($0.15 \times A_0$) on positions and e) 15% of π on phases. Note that the perturbations on positions and velocities are proportional to the collective maximum and not to the individual values. After adding the perturbations we concatenate the solitons and integrate the NLS (1) using a pseudo-spectral method. Additionally, we include a stationary 5% perturbation to the potential and a noise level of 10^{-5} to $u(x, t)$ at *every* time step of the integration (total run is 2.01×10^6

iterations). Fig. 3 depicts the evolution of $u_t(x, t)$ for the unperturbed and the perturbed breather. Despite the large perturbation to the IC and the additive noise, after a brief transient, the breather settles down and retains its localization with an approximate exponential decay (inset b₃). It is interesting to note that stronger perturbations to u did not necessarily destroy the localization but often resulted in a slow excursion of the localized region along the lattice. For breather mobility in nonlinear lattices triggered by perturbations please refer to [21]. The robustness of the localized breather dynamics presented above opens the possibility for experimental corroboration. The large perturbation to the IC results in an initial transient involving radiation loss, which corresponds to a small number of atoms being spilled away from the central cloud and absorbed by the non-condensed atoms at the periphery. After the transient, the breather settles down and retains its localization with an approximate exponential decay (inset b₃). This demonstrates the robustness of the breather to a wide host of perturbations, nonetheless breathers are non-generic in the sense that arbitrary initial conditions do not necessarily produce a breather.

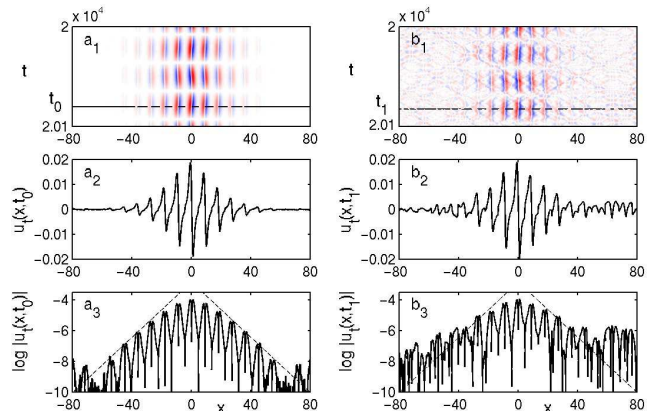


FIG. 3. Robustness of the perturbed localized breather: a) unperturbed and b) perturbed. a₁ and b₁ depict a density plot of $|u_t(x, t)|$. Insets a₂ and a₃ depict $u_t(x, t_0)$ and $\log(|u_t(x, t_0)|)$ at $t = t_0$ (unperturbed) and at $t = t_1$ (perturbed). The times t_0 and t_1 are depicted in a₁ and b₁. Same parameter values as in Fig. 2.

We may use the dynamical reduction described above to devise other breathing phenomena of (1). Within our approximations, any bounded nontrivial orbit of the 2D map M (6) gives rise to complex oscillatory behaviour of the condensates in (1). In particular, periodic points of M correspond to *global* oscillations. The map M has three fixed points: the origin, $F = (x^*, x^*)$ and $F' = (-x^*, -x^*)$, where $x^* = \sqrt{(2-a)/b}$. The fixed points F and F' yield solutions in which all condensates oscillate in phase with the same amplitude x^* . The corresponding global breather for the original system (1) is depicted in Fig. 4.a. Other interesting orbits arise from higher order periodic points. For ex-

ample, the period two orbit $G = -M(G) = M^2(G)$ ($G = (\hat{x}, -\hat{x})$ with $\hat{x}^2 = -(2+a)/b$) corresponds to an amplitude configuration $\{\dots, \hat{x}, -\hat{x}, \hat{x}, -\hat{x}, \dots\}$, ie. anti-phase oscillations (see Fig. 4.b). It is in principle possible to construct more complex patterns for the global oscillations from higher order periodic orbits of the 2D map. An interesting possibility for the dynamics of coupled condensates is the prospect of chaotic evolution. In a neighborhood of the fixed point F there is a region containing chaotic orbits corresponding to chaotic oscillations for the condensates (see Fig. 4.c).

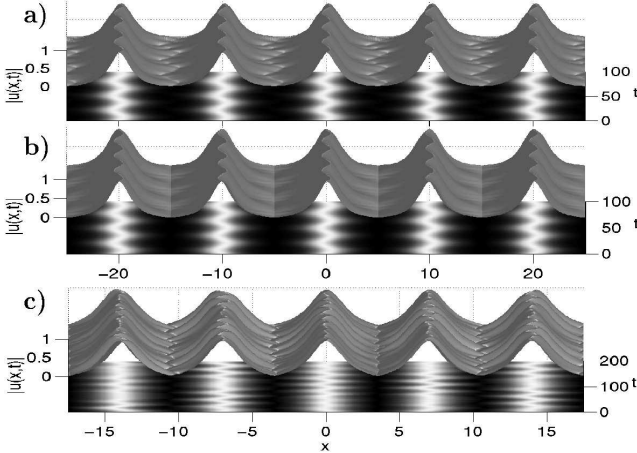


FIG. 4. Global oscillations of the condensates. a) In-phase oscillations corresponding to the nontrivial fixed point F (see Fig. 1). b) Anti-phase oscillations corresponding to a period two cycle of (6) with alternating amplitude sign. c) Chaotic oscillations corresponding to a chaotic orbit of (6).

We have constructed a variety of novel global and localized oscillatory behaviors of BECs in periodic potentials, identifying these solutions with orbits of a reduced 2D map. A key ingredient of the construction of localized oscillations is the existence of a homoclinic tangle. We demonstrate the robustness of these solutions to perturbations. Since BEC experiments are quite delicate, we do not expect that direct manipulation could produce an exact initial condition corresponding to a localized oscillation. Nonetheless, we believe that localized oscillations may be observed in weakly coupled condensates which are appropriately engineered and then permitted to radiate away spurious energy. The techniques presented here can, in principle, be extended to lattices in higher dimensions such as vortex lattices. This has possible implications to modeling the interactions of atoms in optical traps that could potentially be used for quantum computing [22].

We are grateful to J.N. Kutz, B. Deconinck, P.G. Kevrekidis, P. Engels and W.P. Reinhardt for providing stimulating discussions and relevant references. The authors acknowledge support from the Pacific Institute for the Math. Sciences and NSERC grant #611255 during the completion of this work.

-
- * rcarrete@sfu.ca; www.math.sfu.ca/~rcarrete/ric.html.
New address: Dep. of Mathematical and Computer Sciences, San Diego State University, CA 92182-7720.
- [1] B.P. Anderson and M.A. Kasevich, *Science* **282**, 1686 (1998); K. Berg-Sørensen and K. Mølmer, *Phys. Rev. A* **58**, 1480 (1998); D. Jaksch *et al.*, *Phys. Rev. Lett.* **81**, 3108 (1998); A. Trombettoni and A. Smerzi, *Phys. Rev. Lett.* **86**, 2353 (2001).
 - [2] P.S. Jessen and I.H. Deutsch, *Adv. Atom., Mol. Opt. Phys.* **37**, 95 (1996); K.I. Petsas *et al.*, *Phys. Rev. A* **81**, 5173 (1994)
 - [3] E.P. Gross, *Nuovo Cim.* **20**, 454 (1961); L.P. Pitaevskii, *Sov. Phys. JETP* **13**, 451 (1961).
 - [4] A.D. Jackson *et al.*, *Phys. Rev. A* **58**, 2417 (1998); V. Pérez-García *et al.*, *Phys. Rev. A* **57**, 3837 (1998); M. Key *et al.*, *Phys. Rev. Lett.* **84**, 1371 (2000); N.H. Dekker *et al.*, *Phys. Rev. Lett.* **84**, 1124 (2000).
 - [5] P.A. Ruprecht *et al.*, *Phys. Rev. A* **51**, 4704 (1995).
 - [6] J. Reichel *et al.*, *Phys. Rev. Lett.* **83**, 3398 (1999); W. Hänsel *et al.*, *Phys. Rev. Lett.* **86**, 608 (2001); J. Reichel *et al.*, *Appl. Phys. B* **72**, 81 (2000).
 - [7] Th. Busch and J. Anglin, *Phys. Rev. Lett.* **84**, 2298 (2000); S. Burger *et al.*, *Phys. Rev. Lett.* **83**, 5198 (2000).
 - [8] B. Deconinck *et al.*, cond-mat/0106231.
 - [9] M. Schiffer *et al.*, *Appl. Phys. B* **67**, 705 (1998); E.M. Wright *et al.*, *Phys. Rev. A* **63**, 013608 (2001).
 - [10] Collapse for attractive BECs is identified with the collapse of the NLS in dimensions $D \geq 2$. Since the NLS does not blow up in 1D, designing a trap that confines the BEC to an almost perfect 1D profile (a very thin cigar shape) could arrest, or at least delay, collapse.
 - [11] C.C. Bradley *et al.*, *Phys. Rev. Lett.*, **78** 985 (1997); F. Dalfovo *et al.*, *Rev. Mod. Phys.*, **71**, 463 (1999).
 - [12] J.C. Bronski *et al.*, *Phys. Rev. E* (2001) to appear.
 - [13] V.I. Karpman and V. Solov'ev, *Physica D* **3**, 142 (1981).
 - [14] R. Scharf and A.R. Bishop, *Phys. Rev. E* **47**, 1375 (1993); V. Pérez-García *et al.*, *Phys. Rev. Lett.* **77**, 5320 (1996).
 - [15] V.S. Gerdjikov *et al.*, *Phys. Rev. E* **55**, 6039 (1997); J.M. Arnold, *Phys. Rev. E* **60**, 979 (1999).
 - [16] R. Carretero-González and K. Promislow *Discrete and Cont. Dyn. Systems, Series B* (to be published).
 - [17] M. Toda, *Theory of Nonlinear Lattices*. Springer, 1989.
 - [18] J. Denschlag *et al.*, *Science* **287**, 97 (2000).
 - [19] Y.S. Kivshar, *Phys. Rev. E* **48**, R43 (1993); S. Flach and C.R. Willis, *Phys. Rep.* **295**, 181 (1998); T. Bountis *et al.*, *Phys. Lett. A* **268**, 50 (2000).
 - [20] R.S. MacKay and S. Aubry. *Nonlinearity* **7**, 1623 (1994); S. Flach. *Phys. Rev. E* **51**, 1503 (1995); S. Aubry. *Physica D* **71**, 196 (1994).
 - [21] D. Chen *et al.*, *Phys. Rev. Lett.* **77**, 4776 (1996).
 - [22] I.H. Deutsch *et al.*, *Fortschr. Phys.* **48**, 923 (2000).